The Journal of Experimental Biology 202, 2127–2138 (1999)
Printed in Great Britain © The Company of Biologists Limited 1999
JEB2262



# RED MUSCLE ACTIVATION PATTERNS IN YELLOWFIN (*THUNNUS ALBACARES*) AND SKIPJACK (*KATSUWONUS PELAMIS*) TUNAS DURING STEADY SWIMMING

TORRE KNOWER[1,*], ROBERT E. SHADWICK[1], STEPHEN L. KATZ[1,‡], JEFFREY B. GRAHAM[1] AND CLEMENT S. WARDLE[2]

[1]*Marine Biology Research Division, Scripps Institution of Oceanography, University of California, San Diego, La Jolla, CA 92093-0204, USA* and [2]*SOAEFD Marine Laboratory, PO Box 101, Aberdeen AB11 9DB, UK*

*e-mail: tknower@ucsd.edu

‡Present address: Department of Zoology, Duke University, Durham, NC 27708-0325, USA

*Accepted 11 May; published on WWW 19 July 1999*

## Summary

**To learn about muscle function in two species of tuna (yellowfin *Thunnus albacares* and skipjack *Katsuwonus pelamis*), a series of electromyogram (EMG) electrodes was implanted down the length of the body in the internal red (aerobic) muscle. Additionally, a buckle force transducer was fitted around the deep caudal tendons on the same side of the peduncle as the electrodes. Recordings of muscle activity and caudal tendon forces were made while the fish swam over a range of steady, sustainable cruising speeds in a large water tunnel treadmill. In both species, the onset of red muscle activation proceeds sequentially in a rostro-caudal direction, while the offset (or deactivation) is nearly simultaneous at all sites, so that EMG burst duration decreases towards the tail. Muscle duty cycle at each location remains a constant proportion of the tailbeat period (*T*), independent of swimming speed, and peak force is registered in the tail tendons just as all ipsilateral muscle deactivates. Mean duty cycles in skipjack are longer than those in yellowfin. In yellowfin red muscle, there is complete segregation of contralateral activity, while in skipjack there is slight overlap. In both species, all internal red muscle on one side is active simultaneously for part of each cycle, lasting 0.18*T* in yellowfin and 0.11*T* in skipjack. (Across the distance encompassing the majority of the red muscle mass, 0.35–0.65*L*, where *L* is fork length, the duration is 0.25*T* in both species.) When red muscle activation patterns were compared across a variety of fish species, it became apparent that the EMG patterns grade in a progression that parallels the kinematic spectrum of swimming modes from anguilliform to thunniform. The tuna EMG pattern, underlying the thunniform swimming mode, culminates this progression, exhibiting an activation pattern at the extreme opposite end of the spectrum from the anguilliform mode.**

Key words: red muscle, activation, electromyography, steady swimming, tuna, yellowfin, *Thunnus albacares*, skipjack, *Katsuwonus pelamis*.

## Introduction

Scientists have long been intrigued by the mechanics of axial fish locomotion and have pursued its study using two primary approaches. One is hydrodynamic, describing swimming performance based on the effects that the moving body imparts on the surrounding water (e.g. Lighthill, 1969; Webb, 1975), while the other examines features of the body design itself. While inferences about swimming mode can be based on body morphology (e.g. Wainwright, 1983; Westneat et al., 1993), the approach taken in the present study has focused on the dynamic physiology of the fish's swimming mechanism by probing its muscle function. The purpose of this method is to understand how a particular swimming mode results from the sequence of muscle activation along the fish's body and the subsequent interactions between contracting muscle and the body's structural elements.

Two species of tropical tuna were studied: the yellowfin *Thunnus albacares* (Bonnaterre) and the skipjack *Katsuwonus pelamis* (L.). From a design point of view, tunas present a fascinating subject for study because of their ability to excel in two areas that for many vertebrates remain mutually exclusive: they achieve some of the fastest burst speeds known (e.g. yellowfin: 70 km $h^{-1}$; Magnuson, 1978), yet also demonstrate long endurance for sustained swimming (e.g. the bluefin's 9700 km trans-Pacific crossings from Japan to Baja California; Lindsey, 1978). As Joseph et al. (1988) noted, their performance is analogous to both accomplished sprinting and marathon running. The thunniform swimming mode represents one extreme in the spectrum of axial swimming modes exhibited by fishes. Most of the body is held relatively rigid, while lateral movement and thrust production are focused almost exclusively at the high-aspect-ratio lunate tail. The bulk of the muscle mass is concentrated anteriorly, spatially separated from the thrust-producing tail. The overall goal of our research is to understand the dynamic design features of

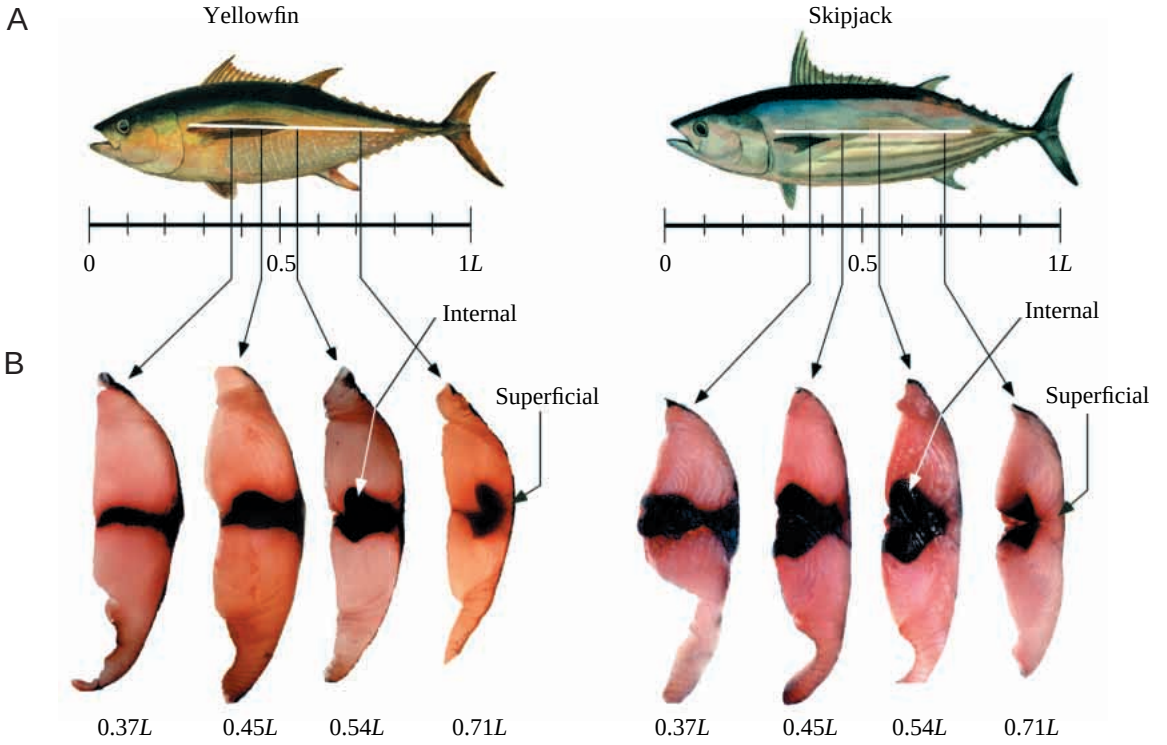


Fig. 1. (A) Side view of a yellowfin tuna and a skipjack tuna showing the longitudinal extent of the internal red muscle (indicated by the white bar) (adapted from paintings by George Mattson in Joseph et al., 1988). (B) Hemi-transverse sections of yellowfin and skipjack muscle, showing the distribution of internal and superficial red muscle. Also shown is the color gradation in the superficial muscle of both species from dark red in the more anterior locations (matching the internal red muscle) to a lighter color at more posterior locations. Views are of anterior faces of slices from the left side of the body. *L*, fork length.

the tuna 'engine' underlying the thunniform propulsion mechanism by analyzing muscle activation patterns and caudal tendon forces in swimming tunas. The present paper focuses on the first component: muscle activation (electromyography). The results from the parallel studies on tendon forces and caudal tendon function will be treated separately.

Some of the physiological features enabling tunas to be such successful pelagic swimmers include a streamlined, fusiform body plan externally and several uncommon anatomical features internally. External features include a smooth skin and recesses for retracting many of the fins, the largest cross-sectional area of muscle mass concentrated near the body's midlength, narrow-necking just forward of the caudal fin for reduced drag, and a large-aspect-ratio lunate caudal fin that provides lift-based thrust (Fig. 1A). Internally, tunas differ from most other fishes in having the bulk of their red muscle located medially, near the backbone (Fig. 1B). This internal mass is an integral part of the nested myotome cones, with the concentric rings of red muscle being continuous with the surrounding white muscle. The myotomes in tunas are highly elongated, which directs the force produced by the anteriorly situated muscle mass rearward to the tail. The unusual anatomical arrangement of the red muscle makes it possible to probe the dynamic function of myotomal cone muscle at steady, cruising speeds without exhausting the fish. This is an attractive feature of studying tunas. In most species of fish, the white muscle is the only avenue for studying the nested myotomes, so prolonged steady swimming conditions are difficult to achieve.

Prior to the present study, the only available data concerning muscle activity in tunas demonstrated the sequential recruitment of aerobic to anaerobic fiber types with increasing swimming speed, as observed in other fishes (Rayner and Keenan, 1967; Brill and Dizon, 1979). However, there is currently no information on the temporal sequence of muscle activation down the body which produces a tail sweep. Because the force-producing muscle mass is separated from the thrust-producing tail, it is important to learn what activation patterns result in this highly specialized swimming mode. To study this, tunas were instrumented with a rostro-caudal series of electromyogram (EMG) electrodes to record electrical activities along the internal red muscle mass as the fish swam in a water tunnel. It was hypothesized that there would still be a discernible traveling wave of activation in the tunas, but that activation of each side would be more nearly instantaneous than in non-thunniform swimmers, which use more undulatory swimming modes. Additionally, yellowfin and skipjack tunas exhibit subtle morphological differences externally and internally (Fig. 1), so another goal of this study was to determine whether these design differences are manifested in

different dynamic behaviors of their muscle. Magnuson (1978) observed that most locomotory adaptations among scombrids appear to be linked to sustained swimming. All scombrids are able to attain fast burst speeds, but the species vary in their capabilities for sustained swimming. Thus, a comparison of EMG patterns in yellowfin and skipjack red muscle could delineate some of these more subtle species differences.

Another anatomical feature distinguishing tunas from most fishes is the presence of thick tendons spanning the peduncle to connect the force-producing muscle mass with the tail. In contrast to most fishes, in which muscle extends all the way to the caudal fin, the posterior myotomes in tunas have been reduced to a series of concentric myoseptal sheaths, forming one superficial and two major deep tendons on each side of the peduncle (the 'great lateral tendon' and the 'intermediate lateral tendons', respectively, of Fierstine and Walters, 1968). This tendon anatomy made it possible to make measurements never before accomplished in any fish: direct measurements of internal muscle forces during swimming, using an 'E'-shaped buckle force transducer fitted around the deep tendons of one side. These measurements permit quantification of the anteriorly generated muscle force reaching the tail for external thrust production. The results of these parallel force studies, conducted in conjunction with the present EMG study, will be the subject of a future paper. For the present report, the time of peak force in each tailbeat was used as a standard reference to normalize muscle activation state from tailbeat to tailbeat.

In summary, by instrumenting yellowfin and skipjack tunas with EMG electrodes and a caudal tendon force transducer, and swimming them over a range of steady, sustained speeds in a water tunnel, we were able (1) to determine the sequential activation patterns down the length of the internal red muscle, (2) to relate these timings to the occurrence of peak force recorded from the tail tendons, (3) to compare the EMGs of yellowfin and skipjack tunas and (4) to compare the EMG patterns of these tunas with those of other fish species to determine whether muscle activation more closely approaches simultaneity (relative to other swimming modes) in this highly specialized, thunniform swimming mode.

## Materials and methods

### *Fish*

All experiments were conducted at the National Marine Fisheries Service, Kewalo Research Facility in Honolulu, Hawaii. Yellowfin *Thunnus albacares* (Bonnaterre) and skipjack *Katsuwonus pelamis* (L.) tunas, ranging in size from 35 to 55 cm fork length (1–2 kg), were caught by local fishermen using barbless hooks and maintained in circular holding tanks (7 m diameter, 1 m deep) with continuous aeration and seawater turnover (temperature range approximately 22–27 °C). Fish were fed daily with chopped squid and allowed to acclimate for at least 1 week before being used in experiments. All care and experimental procedures were conducted in accordance with approved animal protocols.

### *Water tunnel*

The water tunnel has been described previously (originally in Graham et al., 1990; modifications for tunas in Dewar and Graham, 1994a; Graham et al., 1994). Briefly, the 3000 l capacity water tunnel was freshly filled with sea water before each experiment. The water was oxygenated and adjusted to a temperature of approximately 23 °C (near ambient). The working section measured 113 cm×22.5 cm×32.5 cm (length × width × height; cross-sectional area 731 $cm^2$). Water flow speeds were calculated from a regression of voltage output from the propeller motor *versus* output from a flowmeter, as described by Graham et al. (1994). The greatest cross-sectional area of each fish used was less than 10 % of the cross-sectional area of the tunnel's working section; therefore, no water velocity corrections were necessary to compensate for the solid blocking effect of the body.

### *Surgical procedures*

#### *Anesthesia*

A fish was dip-netted from a holding tank and transferred to a plastic bag containing an oxygenated solution of MS-222 [Finquel: methane tricaine sulfonate (Argent Chemical Laboratories), 1:1000 (w/v) in sea water] buffered with either sodium bicarbonate or Tris base (approximately pH 7.8). This served to anesthetize the fish quickly, in order to minimize struggling while it was rushed from the tank to the water tunnel. Surgery was performed in a chamois cradle on top of the working section of the water tunnel while ventilating the fish with a more dilute solution of oxygenated, buffered MS-222 (1:17 500) (Korsmeyer et al., 1997).

#### *EMG methodology*

After the fish had been anesthetized, 2–6 electromyogram (EMG) electrodes were implanted along the length of the internal red muscle (i.e. the red portion of the nested myotome cones, near the backbone; Fig. 1B) of the left side, using a 22 gauge needle. Initially, bipolar hook-type electrodes were used, constructed of 34 gauge Teflon-coated copper wire (Belden Wire and Cable, 8057) with the ends bared 1–2 mm. However, monopolar electrodes (referenced to a common wire implanted under the skin just behind the top of the skull) were used later to take advantage of the much stronger signal-to-noise ratio, which proved very helpful in our difficult field working conditions. Monopolar electrodes were used only after verifying that, with appropriate post-experimental processing, they gave the same burst timings as the bipolar type (see *EMG processing*). After suturing the wires to the skin to prevent slippage, and collecting all the wires into one slim bundle to pass out of the tunnel working section, the electrodes were connected to preamplifiers (Grass Instrument Co., model P15), then amplifiers (Axon Instruments, Inc., CyberAmp 320 or A-M Systems differential a.c. amplifier, model 1700), and the signals were recorded on computer *via* an analog-to-digital (A/D) board (Axon Instruments, Inc., model TL-2). The A/D conversion rate was 500 Hz or (in one experiment) 2000 Hz. Several sampling rates between 500 Hz and 10 kHz were tested

to verify that burst onsets and offsets were not being clipped, and burst durations were equivalent at all these rates. The typical frequency bandwidth for EMG recordings was 30–1000 Hz, which is similar to the range (20–2000 Hz) recommended by Winter (1990).

*Tail tendon force transducer*

The tendon buckle force transducers (designed by A. A. Biewener; Biewener et al., 1988) were constructed as a stainless-steel 'E' shape with a strain gauge mounted on the middle arm and coated with epoxy adhesive to waterproof the leads. All buckles were 15 mm long, but two widths were available (5.0 or 6.5 mm) to accommodate the tendons from different-sized fish. To implant the buckle, a small incision was made in the anesthetized fish just above the fleshy keel on the left side of the peduncle (the same side as the EMG electrodes). The pair of deep lateral tendons on that side were separated from the superficial subcutaneous sheath and threaded through the buckle such that they passed behind the middle arm. The skin was sutured and then externally sealed with tissue adhesive (3M Vetbond) so as to enclose the buckle completely, leaving only the two lead wires to exit the incision. These wires were sutured to the skin near the second dorsal fin and connected outside the tunnel to a strain gauge conditioning amplifier (Measurements Group, Inc., model 2310 or the CyberAmp 320, with the transducer as one-quarter of a Wheatstone bridge) and thence to the computer *via* the A/D interface. Transducers were calibrated on the tendons at the end of each experiment and responded linearly over a range of forces and frequencies exceeding those used by the swimming fish. Quantification of swimming forces is the focus of parallel studies conducted in conjunction with the present EMG study; therefore, details of force calibrations will be described in a separate paper. For the present study, the only analysis required of the transducer signals was to determine the time of peak force within each tailbeat to use as the time reference for standardizing tailbeat-to-tailbeat muscle activation phase.

*Swimming protocols*

After surgery, the MS-222 ventilating solution was replaced with fresh sea water until the fish started to revive, at which point it was lowered into the working section of the water tunnel. The flow was adjusted until the fish swam steadily, which generally took 10–30 min. Recordings were made over the range of speeds at which the individual fish would swim steadily. Using a mirror angled at 45° above the working section, video recordings were made of the fish's dorsal aspect and synchronized with the EMG and force recordings on the computer using the voltage spike from a flashing red diode (visible in the video field). For the present study, the video recordings were used to select sequences of steady swimming for EMG analysis. The selection criteria were that the fish had to be away from the walls and holding station within the flow (i.e. no drifting forwards or backwards or to the left or right) for at least 10 consecutive tailbeats.

At the end of each experiment, the fish was killed by a sharp blow to the head. It was then dissected to verify correct EMG electrode placement in the red muscle, to determine the exact myotome locations of the electrodes, and to verify correct buckle placement on the tendons.

*Analyses*

*Selection criteria*

To obtain the most accurate information possible on muscle activation timing, it was necessary for any given fish to meet all the following criteria before being selected for analysis: steady swimming over a range of water velocities (as demonstrated by consistent beat-to-beat frequencies, while swimming in the center of the flow); correctly placed EMG electrodes with clean signals at several body locations; and a successful tendon force signal. Preliminary analyses were made on six yellowfin and eight skipjack tunas to ascertain how well these criteria were met. Ultimately, the data from four yellowfin (40–44 cm fork length; 1174–1391 g) and three skipjack (38–41 cm; 803–1055 g) were found to satisfy these stringent requirements and are presented in this paper.

*EMG processing*

Our experiments were conducted in highly challenging field working conditions (e.g. the conductive nature of sea water, the length of electrode wires required to reach from the fish to the preamplifiers (approximately 1.5 m) and the proximity of radio towers to the facility). Therefore, after comparative studies using bipolar and monopolar electrodes, we elected to use monopolar electrodes to enhance the signal:noise ratio (while keeping filtering to a minimum to ensure accurate EMG burst timings). However, this method necessitated post-experimental processing to eliminate possible movement artifacts and to clarify burst onsets and offsets (i.e. the times when electrical activity starts and stops). This was performed using AcqKnowledge software (BIOPAC Systems, Inc.), with its finite impulse response (FIR) filters, thresholding and peak detection capabilities. The typical protocol was as follows. For each speed, steady swimming segments of 10–30 consecutive tailbeats were selected from the files on the basis of the video recordings. Each EMG train was first subjected to a high-pass filter (30 Hz cut-off) to eliminate possible movement artifacts, rectified, then put through a low-pass filter (10 Hz cut-off) to define a general envelope for each burst. Finally, a voltage threshold level was set (on the basis of the signature of the high-pass-filtered, rectified signal) so that onset and offset times of the burst envelopes could be selected automatically by the program. These times were then imported into a spreadsheet program (Microsoft Excel) to calculate mean burst durations, relative onset and offset times down the length of the body, and the temporal relationship between muscle activation and peak force registered by the tendon transducer. To allow comparisons among fish, muscle activation onset and offset times were expressed as a proportion of tailbeat period ($T$), using the time of peak force registered by the force transducer as the reference point. It was first verified that the times of peak force in the buckle signals consistently matched

the same kinematic reference in the video recordings, beat-to-beat, irrespective of tailbeat frequency. EMG locations were expressed as proportion of fork length (*L*), with the nose being 0 and the tail fork 1.

*Statistics*

In all plots, error bars represent ± one standard deviation (S.D.), and lines are fitted by least-squares regressions. To assess possible interspecies differences in EMG onset patterns and duty cycles between yellowfin and skipjack tunas, mean values for individual fish were first calculated across speeds. Note that in tunas (see Fig. 4B), as in most fishes studied, EMG duty cycle remains a constant proportion of the tailbeat period, irrespective of swimming speed. A mean slope (or intercept) value was determined from 10–30 consecutive tailbeats per swimming bout for each speed; these speed values were then averaged to derive a speed-independent mean for each individual fish. Subsequently, means for the two species were compared using a *t*-test, using a pooled variance (after verifying using an *F*-test that the variances were not significantly different); *N* represents the number of individuals of each species (*N*=4 for yellowfin; *N*=3 for skipjack). Results are reported in the text and figure legends.

## Results

### *Muscle morphology*

Body plans of a yellowfin tuna and a skipjack tuna (Fig. 1A) show the longitudinal extent and internal position of the red muscle. Transverse sections from each species (Fig. 1B) illustrate the continuity between red and white muscle within the nested cones. In yellowfin, the red muscle near the backbone extends from approximately 0.26*L* to 0.80*L* (largest cross-sectional area at 0.56*L*); in skipjack, it extends from 0.28*L* to 0.77*L* (largest cross-sectional area at 0.50*L*). These ranges are comparable with those found by Graham et al. (1983) in similar-sized specimens: 0.30–0.85*L* in yellowfin and 0.32–0.80*L* in skipjack. In the size range of fish used for the present study, the region in which the red muscle mass was large enough to target consistently with EMG wires was approximately 0.35–0.65*L*.

### *Swimming velocities and tailbeat frequencies*

The data presented are from similarly sized yellowfin and skipjack tunas swimming at sustained speeds powered only by the red, aerobic muscle. In early experiments, EMG electrodes were also implanted into white muscle, but no activity was observed during steady swimming. White muscle activity was observed only when fish gave brief, erratic bursts of swimming.

Although there was variability in the speed range over which individual fish would swim steadily, skipjack typically preferred to swim against faster water velocities than did yellowfin. However, in the range of speeds where skipjack and yellowfin swimming overlapped, the two species used similar tailbeat frequencies for a given water velocity (Fig. 2).

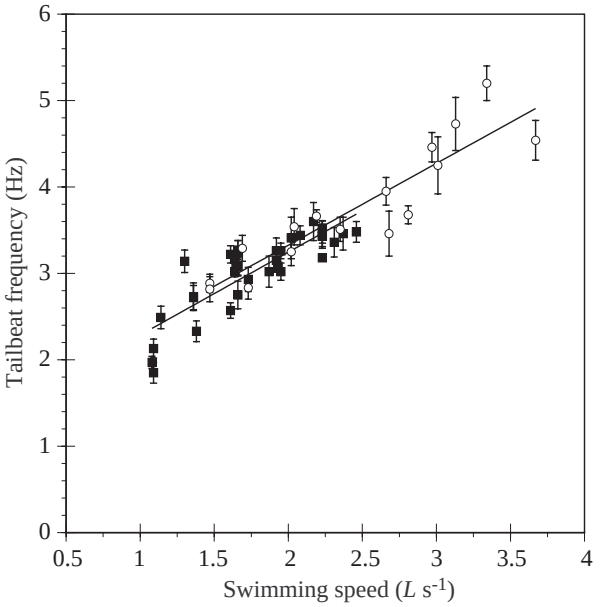


Fig. 2. Tailbeat frequency ($f_{TB}$; Hz) as a function of swimming speed ($v$; $L$ s$^{-1}$, where $L$ is fork length) for four yellowfin (40–44 cm; closed squares) and three skipjack (38–41 cm; open circles). Points represent means and standard deviations of tailbeats within a swimming bout (each bout consists of 10–30 tailbeats). Lines are fitted by least-squares regressions. For skipjack, $f_{TB}$ =0.95$v$+1.43, $P$<0.001, $r^2$=0.83; for yellowfin, $f_{TB}$ =0.96$v$+1.33, $P$<0.001, $r^2$=0.72.

Yellowfin swam at between 46 and 105 cm s$^{-1}$ (1.1–2.5 $L$ s$^{-1}$), using tailbeat frequencies of 1.9–3.6 Hz. The range encompassed by the skipjack, in contrast, was 60–140 cm s$^{-1}$ (1.5–3.7 $L$ s$^{-1}$), with tailbeat frequencies of 2.8–5.2 Hz. The data for both these species fall within the range of tailbeat frequencies found by Dewar (1993) and Dewar and Graham (1994b) for unanesthetized, uninstrumented tunas of comparable size swimming in this same tunnel. Therefore, the surgical procedures and implanted wires appear not to affect adversely the swimming behavior of these fish in this regard. Both species exhibited a linear relationship between tailbeat frequency and swimming speed (Fig. 2), which is typical of steady swimming in many fishes.

### *Electromyography and timing of peak tail tendon forces*

Fig. 3A illustrates 16 consecutive tailbeats of unprocessed EMG signals from the red muscle at 0.40, 0.52 and 0.63*L* in one side of a swimming skipjack tuna. Fig. 3B shows the same at 0.26, 0.43, 0.52 and 0.67*L* during four consecutive tailbeats in a swimming yellowfin, except that time is expanded and the EMG traces have been high-pass-filtered and rectified (showing the first steps in post-experimental processing). In both cases, the force signal from the transducer on the tail tendons (on the same side of the body as the EMG electrodes) is shown at the bottom. The long sequence of steady tailbeats illustrated in Fig. 3A is typical of the prolonged steady swimming bouts routinely recorded from fish in the water tunnel, and which were chosen for analysis. The expanded

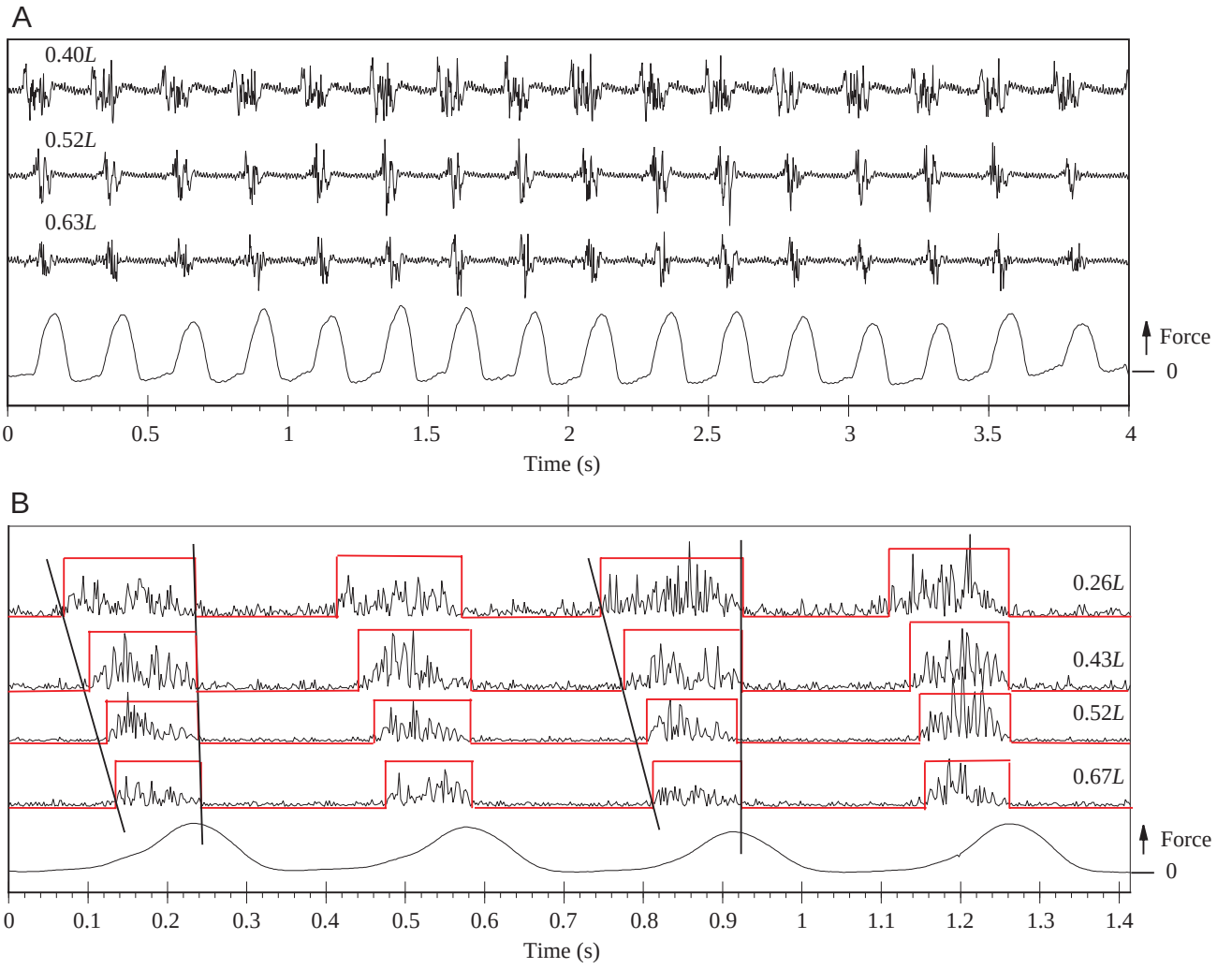


Fig. 3. (A) An example of electromyogram (EMG) traces (with no post-experimental processing) and the tendon buckle force trace from 16 consecutive tailbeats of a 40.7 cm skipjack tuna swimming at $3\,L\,s^{-1}$ (=122 cm $s^{-1}$; $L$ is fork length). The even spacing in time between EMG bursts or force peaks in each trace indicates steady swimming. (B) Expanded view of four tailbeats from a 43 cm yellowfin tuna swimming at $1.8\,L\,s^{-1}$ (=77 cm $s^{-1}$). EMG traces have been high-pass-filtered (30 Hz cut-off) and rectified (the first steps of post-experimental processing). Red square waves indicate detection of burst onsets and offsets. Slanted, solid lines are visual aids to indicate the sequential delay in EMG burst onsets moving posteriorly down the fish's body. The vertical lines show that EMG offset in the muscles is synchronous with peak force at the caudal peduncle. The positions of the EMG traces are scaled on the *y*-axis according to the axial locations on the body.

view of four tailbeats in Fig. 3B facilitates an examination of EMG burst characteristics. The trends are the same for both species: during each tailbeat, the muscle mass on one side is activated sequentially down the length of the fish, the anterior muscles becoming active before those located more posteriorly. The EMG offsets are nearly synchronous, and the force peaks in the ipsilateral tendons just as the muscle activity ceases. The diagonal lines in Fig. 3B indicate that burst duration decreases at more posterior locations on the fish.

When muscle activity is plotted in absolute time at different swimming speeds, it becomes apparent that burst duration at any given location also decreases with increased speed. Fig. 4A shows EMG onset and offset times at different tailbeat frequencies for a 44 cm yellowfin and a 38 cm skipjack. To standardize beat-to-beat EMG timings, the time at which peak force occurred within each cycle was used as the zero time reference, because it had been determined from kinematics that this event always occurs at the same point in the tail sweep, regardless of swimming speed. In Fig. 4A, the time of peak force in the preceding tailbeat is set to 0 s, with the next cycle of EMG activity following. The distance between the onset and offset regression lines (which are extrapolated to the approximate full extent of the red muscle, 0.25–0.80*L*) represents burst duration; the wedge shape illustrates that burst duration decreases posteriorly. In addition, it can be seen that, as the fish swims faster, the slopes of the onset lines become increasingly steep, denoting the increased velocities required to propagate the wave of muscle activation down the body to produce more rapid body undulations. These findings confirm preliminary data reported previously (Knower et al., 1993).

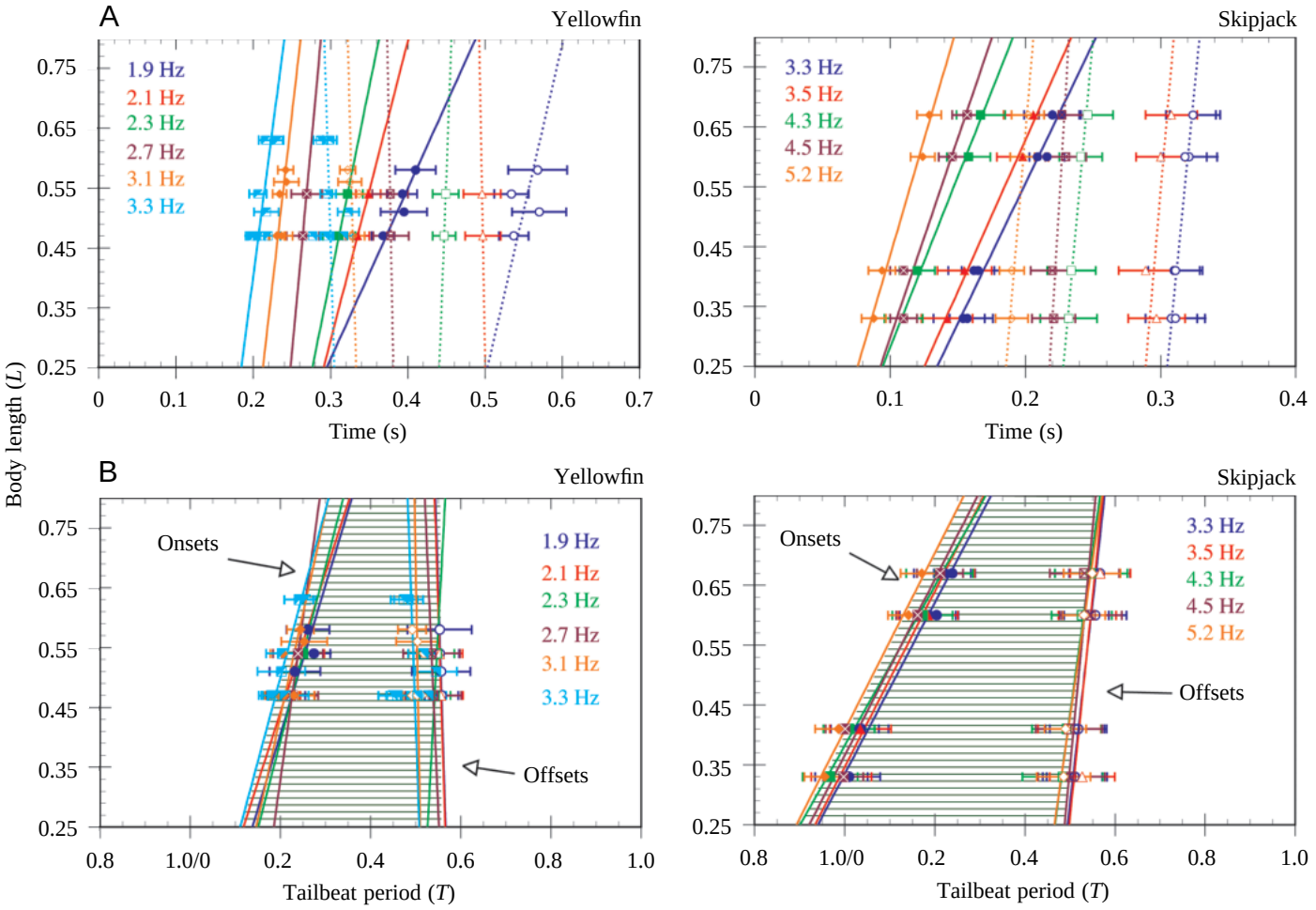


Fig. 4. (A) Electromyogram (EMG) activation onsets (solid lines) and offsets (dotted lines) in the red muscle of one yellowfin (44 cm) and one skipjack (38 cm) at various tailbeat frequencies plotted in absolute time (s) after peak force from the previous tailbeat (=time 0). Note that the onset regression lines at faster speeds have steeper slopes, showing that the EMG trains must travel faster (as expected) to elicit faster tailbeat frequencies. The distance between onset and offset lines represents burst duration. Points are means and standard deviations of tailbeats ($N$=10–30) within a swimming bout. For predictive purposes, regressions have been extrapolated to encompass the entire linear distribution of the red muscle (0.25–0.80$L$). (B) EMG onsets and offsets from A normalized to tailbeat period ($T$). Graphs show approximately one tailbeat cycle, with time of peak force in the tail tendons (on the same side as the EMG electrodes) arbitrarily set to 0.5$T$. Now all the regression lines for the muscle activation sequences are superimposed, demonstrating that muscle activation and deactivation maintain the same phase within the tailbeat cycle, irrespective of swimming speed. For both A and B, all least-squares regressions for onset and offset lines were calculated with time as the dependent variable; axes were then switched to illustrate slopes as length per unit time.

To compare muscle activity from different fish across a range of swimming speeds, it is easier to visualize trends by expressing activation times in terms of duty cycles; i.e. normalized to the period of time required to complete one tailbeat ($T$). Thus, in Fig. 4B (which shows data from the same yellowfin and skipjack as in Fig. 4A), normalized onset and offset times have been plotted relative to the time of peak force on the same side, which has arbitrarily been set at 0.5$T$. In Fig. 4B and in all remaining figures, the time of peak force occurring at the culmination of the EMG sequence within a tailbeat has been used as the standardizing time reference. When $T$=0 and $T$=1, peak force is registered in the tail tendons on the opposite side. Now, muscle activation states at different tailbeat frequencies still show the wedge shape but are superimposed. This demonstrates that, as in other fishes, the duty cycle at a given muscle location on the body remains essentially constant for any cruising speed powered by the red, aerobic muscle. Another way of looking at this is illustrated in Fig. 5, which shows muscle duty cycle as a function of axial position on the body for four yellowfin and three skipjack, across all swimming speeds. On average, the skipjack duty cycles at each location are longer than those of the yellowfin ($t$-test; $P$<0.02).

Fig. 6 combines data from the four yellowfin and three skipjack and also illustrates the relationship between red muscle activation and caudal tendon force development and relaxation. In both species, the anterior muscles are active for longer than the posterior ones, but there is a period when all

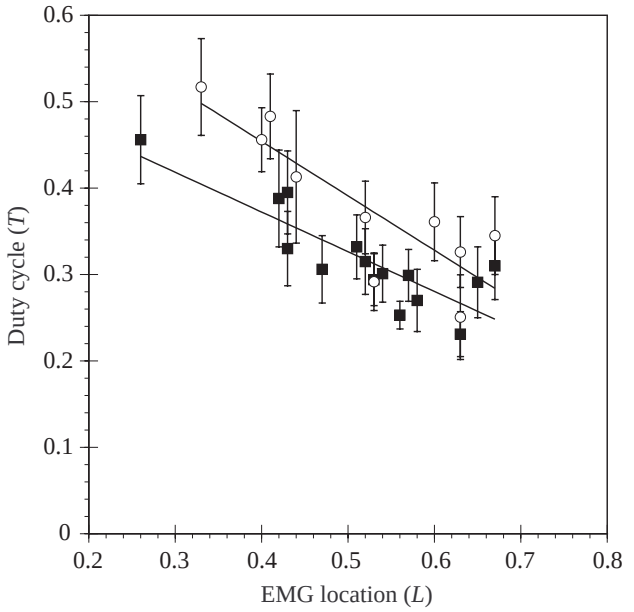


Fig. 5. Electromyogram (EMG) duty cycle (as a proportion of tailbeat period, *T*) in red muscle as a function of muscle location (as a proportion of fork length, *L*) for four yellowfin (closed squares) and three skipjack (open circles) across all swimming speeds (indicated in Fig. 2 for each species). This shows that duty cycles decrease in more caudal locations but that, at any given location, the period of muscle activation remains a constant proportion of the tailbeat cycle, irrespective of tailbeat frequency. Skipjack exhibit somewhat longer duty cycles than yellowfin [*t*-test: slopes are not significantly different ($0.1<P<0.2$), but intercepts are significantly different ($0.01<P<0.02$)]. Yellowfin regression: $y=-0.46x+0.56$ ($r^2=0.71$, $P<0.001$); skipjack regression: $y=-0.63x+0.74$ ($r^2=0.74$, $P=0.001$). Points and error bars are means and standard deviations of all tailbeats from all speeds at each location.

ipsilateral muscle is active simultaneously. Across the distance encompassing the majority of the red muscle (0.35–0.65*L*), simultaneous activation lasts approximately 0.25*T* in both species or 50 % of the duration of one tail sweep. Even when the data are extrapolated to the full extent of the red muscle (measuring the time between activation onset at 0.80*L* and offset at 0.25*L*), all ipsilateral muscle is active for 0.18*T* in yellowfin and for 0.11*T* in skipjack (36 % and 22 %, respectively, of the duration of one tail sweep). In skipjack, muscle activation starts in the anterior muscle slightly before (0.08*T*) peak caudal tendon force is reached on the opposite side, whereas in yellowfin, it starts 0.08*T* after contralateral peak force. Skipjack exhibit a brief overlap between the end of posterior muscle activity on one side and the start of anterior activity on the opposite side (0.15*T* predicted maximum between the extreme ends of the muscle length at 0.25*L* and 0.80*L*), whereas in yellowfin, there is no contralateral overlap in muscle activity. Throughout this paper, muscle 'activity' refers strictly to electrical activity (EMG) in the muscle only.

## Discussion

The overall goal of this research is to understand the physiological design features of the tuna 'engine' that define the thunniform mode of swimming. The present study has for the first time elucidated the temporal patterns of red muscle activation in two species of tuna, providing the foundation for this quest. Invasive measurements on free-swimming tunas have been limited in the past because the high metabolic rates and delicate skin of these endothermic fish make handling and successful anesthesia difficult. Using new surgical procedures developed during this project (and by Korsmeyer et al., 1997), it became possible to instrument fish successfully with several EMG electrodes and a tendon force transducer simultaneously. Using a large water tunnel enabled the recording of measurements from instrumented fish swimming at controlled, steady speeds for hours at a time. This made possible not only a general examination of myotomal cone muscle function during steady swimming but also the first detailed description of the red muscle activation patterns underlying the thunniform swimming mode.

### *Muscle activation in tunas: comparison of yellowfin and skipjack*

The general trends describing sequential muscle activation in yellowfin and skipjack are similar: both species exhibit decreasing duty cycles towards the tail, duty cycle is independent of swimming speed, and peak force in the caudal tendons coincides with near-simultaneous muscle deactivation on that side of the body. However, there are also subtle differences between the two species. As can be seen in Fig. 6, the sequential train of EMG onsets travels down the body faster in the yellowfin than in the skipjack, as shown by the steeper slope of the yellowfin onset regression line. The yellowfin offsets are nearly simultaneous, while the skipjack offsets exhibit a slight rostro-caudal delay. Additionally, the trends indicated in Fig. 5 (and Fig. 6) are that duty cycle at any given muscle location is longer in skipjack than in yellowfin. The combination of these factors results in complete contralateral segregation of muscle activity in yellowfin, but slight activation overlap in skipjack (the anterior muscle at 0.25*L* is predicted to turn on 0.15*T* before activity at 0.80*L* on the opposite side has finished; Fig. 6). Finally, all the muscle on one side is simultaneously active for a greater proportion of the tail sweep in yellowfin than in skipjack (36 % in yellowfin *versus* 22 % in skipjack; Fig. 6).

What are the consequences of these differing EMG patterns on swimming mode? The yellowfin mechanism involves a design that approaches near-synchronous muscle activation (and, hence, force production) on each side and, because there is no overlap in contralateral activity, this suggests that yellowfin use a stiffer swimming mode than skipjack (see below for comparisons with other fishes). Swimming kinematics are dependent on the interaction between muscle activation and body morphology, so EMG patterns are correlated with body design. Skipjack are more elongate than yellowfin, have less body depth, have a smaller tail span and

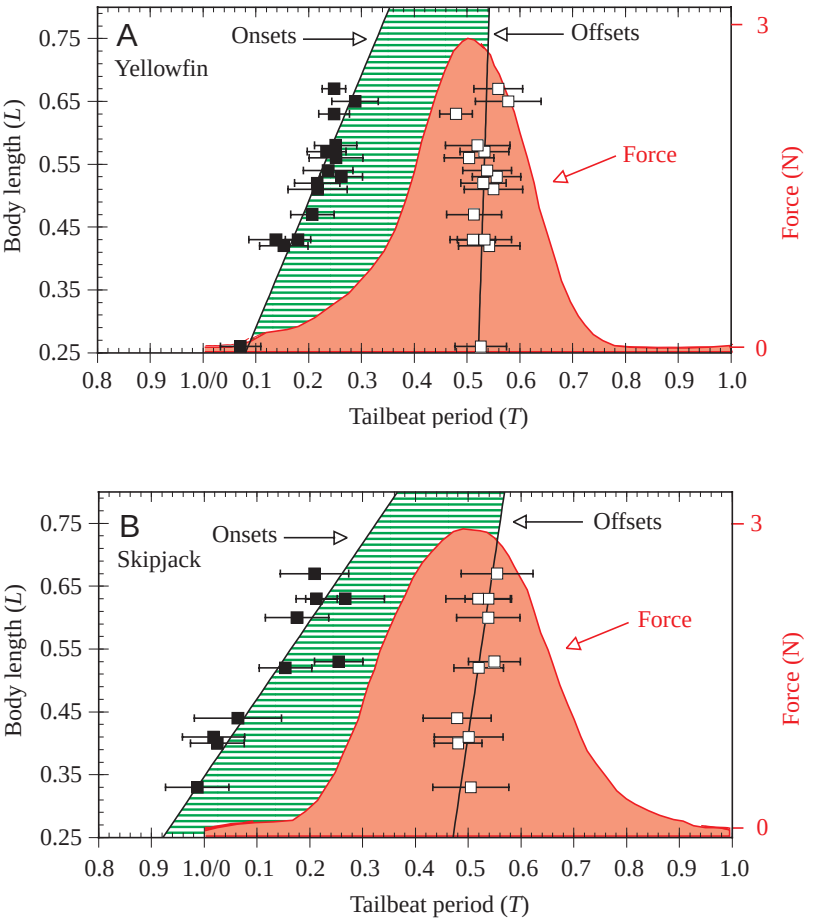


Fig. 6. Summary of red muscle activation data for the four yellowfin (A) and three skipjack (B) tunas across all swimming speeds (see Fig. 2). Superimposed on each plot is a representative trace of force development and relaxation measured by the caudal tendon transducer during one tailbeat to illustrate the timing association between muscle activation and force. The occurrence of peak force in the tail tendons (on the same side of the fish as the recorded electromyograms, EMGs) has been arbitrarily set at 0.5*T*, where *T* is tailbeat period. Kinematically, 0.5*T* is when the tail tip is crossing the swimming track towards the side with the active EMG electrodes. *T*=0 and *T*=1 correspond to peak force on the opposite tail sweep. In both species, peak force is reached just before all the muscle mass on that side is deactivated. The yellowfin show complete segregation of muscle activity between sides, while the skipjack show very slight overlap (the anterior muscles on one side are activated before the contralateral posterior ones are deactivated). Individual points and error bars along the EMG onset and offset regression lines represent means and standard deviations of all tailbeats from all speeds at that location (10–30 tailbeats per swimming bout per speed; 3–8 speeds per fish). Yellowfin onset regression: $y=1.73x+0.15$ ($r^2=0.86$, $P<0.001$); skipjack onset regression: $y=1.0x+0.38$ ($r^2=0.81$, $P<0.001$). The slope of the yellowfin onset regression line is significantly different from that for the skipjack; *t*-test, $0.01<P<0.02$. As in Fig. 4, analyses were performed with EMG time as the dependent variable; axes were then switched to portray data in terms of length per unit time.

area (Magnuson, 1978), and have much smaller pectoral fins (Fig. 1). The last point is particularly pronounced in the size range of fish used for this study: small yellowfin have much larger pectoral fins relative to their body size than do skipjack and therefore derive more hydrodynamic lift (Beamish, 1978). Consequently, skipjack require a faster minimum swimming velocity to maintain hydrostatic equilibrium (Fig. 2). The fact that these two tuna species have subtle differences in their body morphologies and swimming kinematics may explain some of the equally subtle differences observed in the EMG patterns. In summary, although these two tuna species are similar, their morphological design differences appear to be correlated with dynamic design differences in muscle activation patterns and, ultimately, swimming mode.

*Muscle activation in tunas compared with other species of fish*

A persistent question in studies of axial fish locomotion in any species is whether each entire myotome is activated as a unit or whether muscle is activated more according to the longitudinal position of the vertebral segments. For example, Jayne and Lauder (1995b) found that in largemouth bass (*Micropterus salmoides*), the central portion of each myotome (white muscle) was activated simultaneously as a unit during burst-and-glide swimming. In the present tuna study, one experiment was performed in which an array of EMG electrodes was implanted across a transverse plane of red muscle myotomes at two axial locations (in a yellowfin). Because the muscle activation wave travels so quickly in tunas, and the myotomes are so thin (1–2 mm), our data are currently insufficient to resolve conclusively whether myotomes are activated wholly or in part. However, while whole-myotome recruitment cannot be ruled out, the EMG progressions observed in all other experiments, taken in consideration with the myotome morphology, indirectly support the idea that red muscle activation is under segmental neuronal control (i.e. more according to axial position). In all experiments, a sequential train of EMG onset times was consistently recorded down the body, irrespective of which myotome rings the electrodes were in (determined by *post mortem* dissections). The extremely elongated myotomes in these species span a maximum of 13 (yellowfin) or 17 (skipjack) vertebrae (T. Knower, personal observations), which makes it unlikely that the electrodes would always have been implanted in separate myotomes along the fish's body. Supposing that each myotome were activated as a unit, one would then expect to observe non-sequential patterns of rostro-caudal activation in at least some of the experiments (e.g. more posterior locations being activated prior to anterior ones), but such patterns were not observed. In addition, Altringham and Block (1997) found evidence in yellowfin tuna that intrinsic muscle twitch characteristics appear to vary according to distance from the backbone (but not consistent with different myotomes).

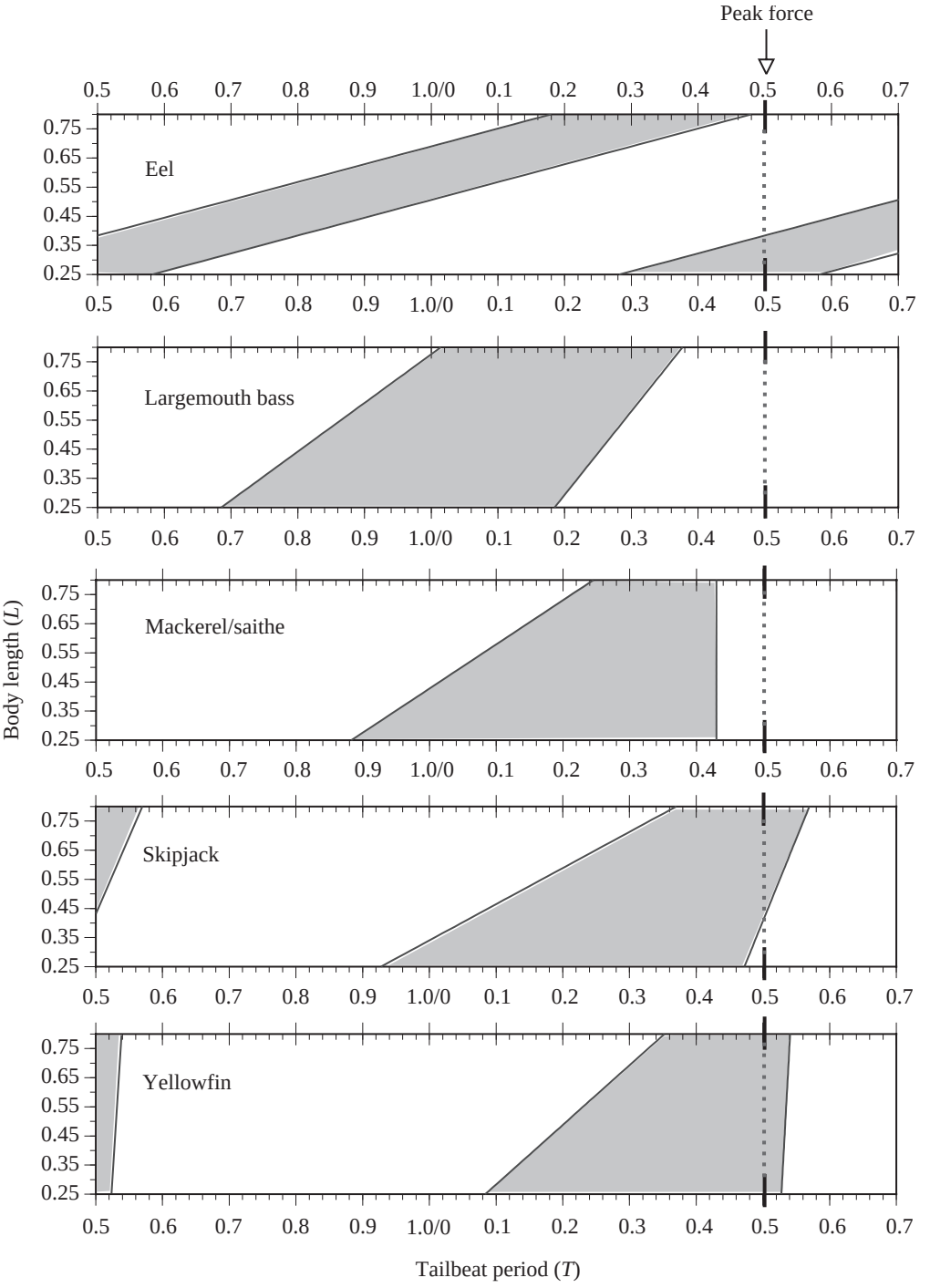


Fig. 7. Comparison of tuna internal red muscle activation with superficial red muscle activation from other species representing anguilliform, subcarangiform and carangiform swimmers. Shaded wedges indicate activity during one tail sweep (=half a cycle), with peak force (or when the tail tip crosses the swimming track towards the active side) for that sweep set arbitrarily at 0.5*T*, where *T* is tailbeat period. For further kinematic reference: at 0.25*T*, the tail tip is at its farthest lateral extreme on the side opposite the recorded electromyograms (EMGs); at 0.75*T*, the tip is at its farthest lateral excursion on the side containing the EMG electrodes; and at *T*=0 and *T*=1, the tip is crossing the swimming track away from the side of the recorded EMGs. The ordinate range corresponds to the longitudinal extent of internal red muscle in the tunas. Tuna data are the regressions from Fig. 6; data for the other species were derived from the following: eel *Anguilla rostrata* (0.75–1.0 L $s^{-1}$; not all muscle anterior to 0.45*L* is active at speeds slower than 0.75 *L* $s^{-1}$), G. B. Gillis, personal communication and Gillis (1998); largemouth bass *Micropterus salmoides* (2.4 *L* $s^{-1}$), Jayne and Lauder (1995a,c); mackerel (*Pollachius virens*)/ saithe (*Scomber scombrus*) (1.8–13 Hz/1.9–7.5 Hz; 0.7–1.0*L*/*T*), Wardle and Videler (1993). *L* is fork length in all species except eel, where it is total length.

Certainly, with the large number of motoneurons supplying any single myotome (Bone, 1978; Johnston, 1983; Jayne and Lauder, 1995b), many different activation patterns are conceivable in different fish species. In these tunas, each myotome has both red and white muscle components, which already necessitates multiple innervation because white muscle is not active at slow speeds. The myotomal cone structure of tuna red muscle affords a unique opportunity to probe muscle activation at sustained, steady swimming speeds. Further studies, preferably in larger individuals, are necessary to elucidate definitively the neuronal control of tuna muscle activation.

Having ascertained the temporal course of red muscle activation in yellowfin and skipjack, it is possible to make predictions about the thunniform swimming mode on the basis of comparisons with EMG data from other fish species. In 1926, Breder published a now-familiar classification scheme for describing different swimming modes on the basis of the kinematics of movement. For fishes that swim by axial locomotion, this scheme describes a progression from fish

without tail blades, which use whole-body undulations to press against the water (anguilliform swimmers), to those employing less undulatory movements, in which most thrust is developed at the posterior end of the body (carangiform swimmers) (Lindsey, 1978; Webb, 1998). At the extreme end of the spectrum from anguilliform swimmers, the thunniform swimmers (e.g. tunas; sharks in the family *Lamnidae*) exploit a lift-based propulsion mechanism in which thrust is generated almost exclusively by oscillation of a lunate tail (Lighthill, 1969; Webb, 1998). The kinematic details of these swimming modes are dependent on parameters such as muscle activation pattern, body morphology and physical interactions with the water. It turns out that many of these underlying components, including EMG patterns, also show a recognizable progression of trends, parallel to the kinematic spectrum. Several authors have reviewed EMG patterns found in anguilliform, subcarangiform and carangiform fishes (e.g. Videler, 1993; Wardle and Videler, 1994; van Leeuwen, 1995; Wardle et al., 1995; Gillis, 1996; Jayne and Lauder, 1996; Hammond et al., 1998; Shadwick et al., 1998). For comparison, data from a few representative species are presented with the tuna data in Fig. 7.

To standardize EMG times within a tailbeat cycle, the time of peak force production at the tail was again used as the reference. For the tunas, this reference was provided directly by the buckle force transducer on the caudal tendons. To transform EMG data from other species in the literature, a kinematic reference for peak force was used, based on the assumption that this event occurs as the tail tip sweeps across the swimming track, i.e. at 0.5*T* (as predicted by Lighthill, 1971; Wardle, 1985). Activation patterns during cruising swimming are presented from the aerobic muscle on one side only. The examples shown are representative of anguilliform (eel), subcarangiform (largemouth bass), carangiform (mackerel/saithe) and thunniform (skipjack and yellowfin tunas) swimmers.

Several patterns emerge across this spectrum. With changes in swimming mode from whole-body undulations to tail oscillations come decreasing duty cycles at more posterior body locations and decreasing levels of simultaneous contralateral muscle activity. The tuna EMG patterns culminate this progression by further separating the activity between left and right sides. Progressing from anguilliform to thunniform swimming, burst duration grades from being nearly constant down the length of the body (eel) to being long rostrally and short caudally (mackerel, tunas). Also, muscle activation begins earlier within the tailbeat in swimming modes that involve more of a propulsive wave on the body (eel, bass), and there is a greater degree of simultaneous activity on both sides (at different longitudinal sites). With a progression to stiffer modes of swimming, in which most body motion is concentrated near the tail (mackerel, tunas), there is less overlap in activity between sides: EMG onsets begin later in the tailbeat cycle, while burst offsets at all locations become more nearly synchronous and coincide more closely with the time of peak force.

The trend in dynamic swimming design towards simultaneity of muscle activation (and force production) culminates in the yellowfin tuna swimming design, in which there is a long portion of the tail sweep during which all muscle is active, resulting from complete contralateral segregation of activity. As a result, body undulation forward of the tail is minimized. Because the force-generating 'engine' is spatially separated from the thrust-producing 'propeller', this activation mechanism, in combination with the extremely elongated myotomes, serves to deliver a coordinated instant of maximum thrust rearward to the tail *via* the caudal tendons. This pattern of muscle activation is at the opposite extreme from the anguilliform pattern and underlies the highly specialized thunniform swimming mode that allows tunas to achieve such remarkable swimming performance.

We gratefully thank G. B. Gillis for providing the EMG data for *Anguilla*, A. A. Biewener for getting us started with the tendon buckles and providing the stainless-steel templates, J. Enright for invaluable guidance on statistics, and the Inter-American Tropical Tuna Commission for permission to duplicate and modify the tuna paintings used in Fig. 1A. We also thank K. Korsmeyer, H. Dewar and N. C. Lai for helping with the swimming experiments, R. Brill, R. Sumida and S. Yano for support at the NMFS Kewalo Research Facility, the captain and crew of the F/V *Corsair*, M. Latz for the use of his scanner and M. C. Clifton and B. Boyd for electronics assistance. R. Lieber, G. Lutz, J. Nauen, G. Szulgit and S. Rapoport made helpful suggestions on the manuscript, as did two anonymous reviewers. This research was supported by National Science Foundation grants OCE91-03739 and IBN95-14203, the Scripps Institution of Oceanography Tuna Endowment, the Scripps Institution of Oceanography Graduate Department (T.K.), the University of California, San Diego Academic Senate and the San Diego chapter of Sigma Xi (T.K.). C.S.W. received support from the Royal Society to conduct research in Honolulu.

## References

**Altringham, J. D. and Block, B. A.** (1997). Why do tuna maintain elevated slow muscle temperatures? Power output of muscle isolated from endothermic and ectothermic fish. *J. Exp. Biol*. **200**, 2617–2627.

**Beamish, F. W. H.** (1978). Swimming capacity. In *Fish Physiology*, vol. VII (ed. W. S. Hoar and D. J. Randall), pp. 101–187. New York: Academic Press.

**Biewener, A. A., Blickhan, R., Perry, A. K., Heglund, N. C. and Taylor, C. R.** (1988). Muscle forces during locomotion in kangaroo rats: force platform and tendon buckle measurements compared. *J. Exp. Biol.* **137**, 191–205.

**Bone, Q.** (1978). Locomotor muscle. In *Fish Physiology*, vol. VII (ed. W. S. Hoar and D. J. Randall), pp. 361–424. New York: Academic Press.

**Breder, C. M.** (1926). The locomotion of fishes. *Zoologica* **4**, 159–297.

**Brill, R. W. and Dizon, A. E.** (1979). Red and white muscle fibre

activity in swimming skipjack tuna, *Katsuwonus pelamis* (L.). *J. Fish Biol.* **15**, 679–685.

**Dewar, H.** (1993). Studies of tropical tuna swimming performance: thermoregulation, swimming mechanics and energetics. PhD dissertation, Scripps Institution of Oceanography, University of California, San Diego.

**Dewar, H. and Graham, J. B.** (1994a). Studies of tropical tuna swimming performance in a large water tunnel. I. Energetics. *J. Exp. Biol.* **192**, 13–31.

**Dewar, H. and Graham, J. B.** (1994b). Studies of tropical tuna swimming performance in a large water tunnel. III. Kinematics. *J. Exp. Biol.* **192**, 45–59.

**Fierstine, H. L. and Walters, V.** (1968). Studies in locomotion and anatomy of scombroid fishes. *Mem. S. Calif. Acad. Sci.* **6**, 1–31.

**Gillis, G. B.** (1996). Undulatory locomotion in elongate aquatic vertebrates: anguilliform swimming since Sir James Gray. *Am. Zool.* **36**, 656–665.

**Gillis, G. B.** (1998). Neuromuscular control of anguilliform locomotion: patterns of red and white muscle activity during swimming in the American eel *Anguilla rostrata*. *J. Exp. Biol*. **201**, 3245–3256.

**Graham, J. B., Dewar, H., Lai, N. C., Korsmeyer, K. E., Fields, P. A., Knower, T., Shadwick, R. E., Shabetai, R. and Brill, R. W.** (1994). Swimming physiology of pelagic fishes. In *Mechanics and Physiology of Animal Swimming* (ed. L. Maddock, Q. Bone and J. M. V. Rayner), pp. 63–74. Cambridge: Cambridge University Press.

**Graham, J. B., Dewar, H., Lai, N. C., Lowell, W. R. and Arce, S. M.** (1990). Aspects of shark swimming performance determined using a large water tunnel. *J. Exp. Biol.* **151**, 175–192.

**Graham, J. B., Koehrn, F. J. and Dickson, K. A.** (1983). Distribution and relative proportions of red muscle in scombrid fishes: consequences of body size and relationships to locomotion and endothermy. *Can. J. Zool.* **61**, 2087–2096.

**Hammond, L., Altringham, J. D. and Wardle, C. S.** (1998). Myotomal slow muscle function of rainbow trout *Oncorhynchus mykiss* during steady swimming. *J. Exp. Biol*. **201**, 1659–1671.

**Jayne, B. C. and Lauder, G. V.** (1995a). Speed effects on midline kinematics during steady undulatory swimming of largemouth bass, *Micropterus salmoides*. *J. Exp. Biol.* **198**, 585–602.

**Jayne, B. C. and Lauder, G. V.** (1995b). Are muscle fibers within fish myotomes activated synchronously? Patterns of recruitment within deep myomeric musculature during swimming in largemouth bass. *J. Exp. Biol.* **198**, 805–815.

**Jayne, B. C. and Lauder, G. V.** (1995c). Red muscle motor patterns during steady swimming in largemouth bass: effects of speed and correlations with axial kinematics. *J. Exp. Biol.* **198**, 1575–1587.

**Jayne, B. C. and Lauder, G. V.** (1996). New data on axial locomotion in fishes: how speed affects diversity of kinematics and motor patterns. *Am. Zool.* **36**, 642–655.

**Johnston, I. A.** (1983). Dynamic properties of fish muscle. In *Fish Biomechanics* (ed. P. W. Webb and D. Weihs), pp. 36–67. New York: Praeger Publishers.

**Joseph, J., Klawe, W. and Murphy, P.** (1988). *Tuna and Billfish – Fish Without a Country*. La Jolla: Inter-American Tropical Tuna Commission.

**Knower, T., Shadwick, R. E., Wardle, C. S., Korsmeyer, K. E. and Graham, J. B.** (1993). The timing of red muscle activation in swimming tuna. *Am. Zool.* **33**, 30A.

**Korsmeyer, K. E., Lai, N. C., Shadwick, R. E. and Graham, J. B.** (1997). Heart rate and stroke volume contributions to cardiac output in swimming yellowfin tuna: response to exercise and temperature. *J. Exp. Biol.* **200**, 1975–1986.

**Lighthill, M. J.** (1969). Hydromechanics of aquatic animal propulsion. In *Annual Review of Fluid Mechanics*, vol. 1 (ed. W. R. Sears and M. Van Dyke), pp. 413–446. Palo Alto: Annual Reviews, Inc.

**Lighthill, M. J.** (1971). Large amplitude elongated-body theory of fish locomotion. *Proc. R. Soc. Lond. B* **179**, 125–138.

**Lindsey, C. C.** (1978). Form, function and locomotory habits in fish. In *Fish Physiology*, vol. VII (ed. W. S. Hoar and D. J. Randall), pp. 1–100. New York: Academic Press.

**Magnuson, J. J.** (1978). Locomotion by scombrid fishes: hydromechanics, morphology and behavior. In *Fish Physiology*, vol. VII (ed. W. S. Hoar and D. J. Randall), pp. 239–313. New York: Academic Press.

**Rayner, M. D. and Keenan, M. J.** (1967). Role of red and white muscles in the swimming of the skipjack tuna. *Nature* **214**, 392–393.

**Shadwick, R. E., Steffensen, J. F., Katz, S. L. and Knower, T.** (1998). Muscle dynamics in fish during steady swimming. *Am. Zool*. **38**, 755–770.

**van Leeuwen, J. L.** (1995). The action of muscles in swimming fish. *Exp. Physiol.* **80**, 177–191.

**Videler, J. J.** (1993). *Fish Swimming*. London: Chapman & Hall.

**Wainwright, S. A.** (1983). To bend a fish. In *Fish Biomechanics* (ed. P. W. Webb and D. Weihs), pp. 68–91. New York: Praeger Publishers.

**Wardle, C. S.** (1985). Swimming activity in marine fish. In *Physiological Adaptations of Marine Animals* (ed. M. Laverack), pp. 521–540. Cambridge: Company of Biologists Ltd.

**Wardle, C. S. and Videler, J. J.** (1993). The timing of the EMG in the lateral myotomes of mackerel and saithe at different swimming speeds. *J. Fish Biol.* **42**, 347–359.

**Wardle, C. S. and Videler, J. J.** (1994). The timing of lateral muscle strain and EMG activity in different species of steadily swimming fish. In *Mechanics and Physiology of Animal Swimming* (ed. L. Maddock, Q. Bone and J. M. V. Rayner), pp. 111–118. Cambridge: Cambridge University Press.

**Wardle, C. S., Videler, J. J. and Altringham, J. D.** (1995). Tuning into fish swimming waves: body form, swimming mode and muscle function. *J. Exp. Biol.* **198**, 1629–1636.

**Webb, P. W.** (1975). *Hydrodynamics and Energetics of Fish Propulsion*. Ottawa: Department of the Environment, Fisheries and Marine Service.

**Webb, P. W.** (1998). Swimming. In *The Physiology of Fishes*, 2nd edition (ed. D. H. Evans), pp. 3–24. Boca Raton: CRC Press.

**Westneat, M. W., Hoese, W., Pell, C. A. and Wainwright, S. A.** (1993). The horizontal septum: mechanisms of force transfer in locomotion of scombrid fishes (Scombridae, Perciformes). *J. Morph.* **217**, 183–204.

**Winter, D. A.** (1990). *Biomechanics and Motor Control of Human Movement*. New York: John Wiley & Sons, Inc.